

Multi-UAV Pursuit-Evasion with Online Planning in Unknown Environments by Deep Reinforcement Learning

Jiayu Chen^{1,*}, Chao Yu^{1,*✉}, Guosheng Li¹, Wenhao Tang¹, Xinyi Yang¹,
Botian Xu², Huazhong Yang¹, Yu Wang^{1✉}

Abstract— Multi-UAV pursuit-evasion, where pursuers aim to capture evaders, poses a key challenge for UAV swarm intelligence. Multi-agent reinforcement learning (MARL) has demonstrated potential in modeling cooperative behaviors, but most RL-based approaches remain constrained to simplified simulations with limited dynamics or fixed scenarios. Previous attempts to deploy RL policy to real-world pursuit-evasion are largely restricted to two-dimensional scenarios, such as ground vehicles or UAVs at fixed altitudes. In this paper, we address multi-UAV pursuit-evasion by considering UAV dynamics and physical constraints. We introduce an evader prediction-enhanced network to tackle partial observability in cooperative strategy learning. Additionally, we propose an adaptive environment generator within MARL training, enabling higher exploration efficiency and better policy generalization across diverse scenarios. Simulations show our method significantly outperforms all baselines in challenging scenarios, generalizing to unseen scenarios with a 100% capture rate. Finally, we derive a feasible policy via a two-stage reward refinement and deploy the policy on real quadrotors in a zero-shot manner. To our knowledge, this is the first work to derive and deploy an RL-based policy using collective thrust and body rates control commands for multi-UAV pursuit-evasion in unknown environments. The open-source code and videos are available at <https://sites.google.com/view/pursuit-evasion-rl>.

I. INTRODUCTION

Multi-UAV pursuit-evasion, where teams of pursuers attempt to capture evaders while the evaders employ evasive strategies to avoid capture, is a key application of UAV swarms. Multi-UAV pursuit-evasion has important applications in both military and civilian contexts, including UAV defense systems [1], adversarial drone engagements [2], and search-and-rescue [3].

Traditional approaches to solving pursuit-evasion games, such as game theory [4], control theory [5], [6], [7], [8], [9], [10], and heuristic methods [11], [12], [13], face significant limitations when applied to complex real-world scenarios. These methods require accurate and reasonable knowledge of models and initial conditions [14], which may struggle to handle the nonlinear dynamics and high-dimensional environments typically encountered in practical applications.

* Equal contribution.

✉ Corresponding Authors. {yuchao, yu-wang}@tsinghua.edu.cn

¹Department of Electronic Engineering, Tsinghua University, Beijing, 100084, China.

² Work done as an intern in Tsinghua University

This research was supported by National Natural Science Foundation of China (No.62406159, 62325405), China Postdoctoral Science Foundation under Grant Number GZC20240830, 2024T170496.

As a result, researchers have increasingly turned to artificial intelligence (AI) techniques, with reinforcement learning (RL) emerging as a leading solution[15], [16], [17], [18], [19]. RL enables UAVs to iteratively learn pursuit and evasion strategies by interacting with simulated environments. By leveraging neural networks, RL can model complex, cooperative behaviors and discover strategies that are difficult to encode using explicit rules.

However, despite these advancements, most RL-based methods for pursuit-evasion focus on simplified tasks in simulation [20], [21], [22], [23], [24]. These methods frequently model agents, both pursuers and evaders, as point masses or with limited kinematic properties, developing only high-level strategies. Such abstractions overlook the kinematic and dynamic constraints of real-world systems, limiting the effectiveness of these strategies outside simulation environments. Moreover, many RL approaches are tailored to fixed, predefined scenarios, reducing their ability to generalize to diverse and unknown scenarios [15], [20], [25]. Although recent work has explored deploying RL-based pursuit-evasion strategies in real-world settings [26], [25], [9], [27], these efforts have primarily been restricted to two-dimensional tasks, such as ground vehicles or UAVs constrained to fixed altitudes, without addressing the complexities of real three-dimensional environments.

This paper aims to learn an RL policy for multi-UAV pursuit-evasion, perform online planning in unknown environments, and deploy it on real UAVs. The problems are:

- **Joint optimization of planning and control:** UAV actions must be coordinated to capture the evader under partial observation, while avoiding environmental obstacles, preventing collisions, and adhering to dynamics model and physical constraints for safe and feasible flight.
- **Large exploration space:** The 3D nature of UAVs, combined with varying scenarios, significantly expands the state space, resulting in a large number of samples required to find viable strategies using RL.
- **Policy generalization:** RL strategies that are optimized for specific scenarios often fail to generalize to new environments.
- **Sim-to-real transfer:** The sim-to-real gap, a common issue in RL, is particularly pronounced in multi-UAV pursuit-evasion tasks due to the physical constraints of UAVs and the need for agile, precise maneuvers.

We address these challenges by incorporating dynamics

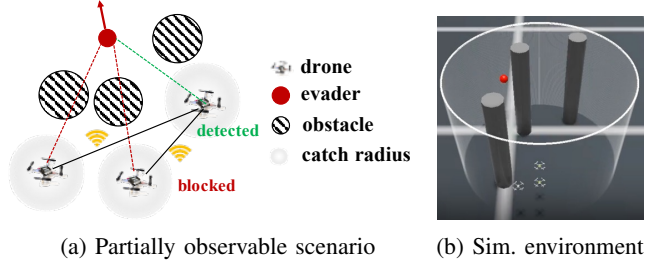
models and physical constraints into training policy for multi-UAV pursuit-evasion tasks. The RL-based policy generates collective thrust and body rates (CTBR) control commands, balancing maneuverability, cooperative decision-making, and sim-to-real transfer. We propose an attention-based, evader-prediction-enhanced network that integrates predictive information about the evader's movements into the RL policy inputs, improving the ability to cooperatively capture the evader with partial observation. Additionally, we introduce an adaptive environment generator to MARL training, which automatically generates diverse and appropriately challenging curricula. This boosts sample efficiency and enhances policy generalization to unseen scenarios.

We evaluate performance across four test scenarios, with results showing that our method outperforms all baselines with a clear margin and maintains a 100% capture rate in unseen scenarios, demonstrating strong generalization. Ablation studies show our approach improves sample efficiency by over 50%. Finally, we employ a two-stage reward refinement process to ensure the policy adheres to physical constraints and deploy it on real Crazyflie quadrotors in a zero-shot manner. To the best of our knowledge, this is the first RL policy with CTBR commands that accounts for dynamics models and physical constraints in pursuit-evasion tasks and can be deployed directly on real quadrotors in unknown environments. The open-source code and videos can be found on our website <https://sites.google.com/view/pursuit-evasion-rl>.

II. RELATED WORK

In pursuit-evasion games, one or more pursuers aim to capture one or more evaders, while the evaders actively avoid capture, distinguishing this from search strategies where the target is passive[28]. Traditional research in this area can be broadly categorized into game-theoretic, control-theoretic, and heuristic approaches[14]. Game-theoretic methods simplify the problem into mathematical models, primarily focusing on differential games[4]. Control-theoretic approaches model the nonlinear dynamics of the pursuit, optimizing strategies using the Hamilton-Jacobi-Isaacs equation[5], [6], [7]. Heuristic methods design forces to guide pursuers—such as attraction to the evader and repulsion from teammates and obstacles—and often utilize optimization techniques like particle swarm optimization (PSO)[10] and artificial potential fields (APF)[13]. However, these traditional methods have limitations in real-world applications due to the gap between their simple system modelling and real UAVs, and the difficulty of handling complex cooperative strategies.

Reinforcement learning (RL) has emerged as a powerful data-driven approach for solving multi-agent coordination problems in pursuit-evasion games[25], [20], [21], [22], [23], [24]. Several studies have applied RL to enhance traditional methods[25] or address issues such as varying agent numbers[21], efficient communication[20], and credit assignment[29]. However, most RL research remains limited to simplified simulation environments, where agents are modeled as particles or constrained by limited kinematics,



(a) Partially observable scenario

(b) Sim. environment

Fig. 1: Setup of multi-UAV pursuit-evasion.

reducing the effectiveness of these strategies in real-world scenarios. While recent work has explored deploying RL-based strategies in pursuit-evasion tasks[26], [25], [9], [27], these efforts have largely been confined to two-dimensional environments, such as ground vehicles, surface vehicles or UAVs at fixed altitudes.

In this paper, we consider the UAV dynamics model and physical constraints, introducing an evader-prediction enhanced network and an adaptive environment generator to address the challenges of large exploration space and policy generalization to unseen scenarios. The learned RL policy is capable of zero-shot deployment to real quadrotors.

III. PRELIMINARY

A. Pursuit-evasion Problem

As shown in Fig. 1a, the multi-UAV pursuit-evasion problem involves N UAVs chasing a faster evader in an obstacle-filled environment. The UAVs aim to capture the evader quickly while avoiding obstacles. The evader is captured if it comes within the capture radius of a UAV. Detection is possible only if no obstacles block the line of sight. When detected, the UAV can pass information to its teammates. The evader, controlled using a potential field method [27], experiences repulsive forces from UAVs, obstacles, and arena boundaries, with force inversely proportional to distance.

B. Problem Formulation

We formulate the multi-UAV pursuit-evasion task as decentralized, partially observable Markov decision processes (Dec-POMDPs), $M = \langle \mathcal{N}, \mathcal{S}, \mathcal{A}, \mathcal{O}, \mathcal{S}_0, \mathcal{P}, \mathcal{R}, \gamma \rangle$ with the state space \mathcal{S} , the joint action space \mathcal{A} , the observation space \mathcal{O} , the space of initial states \mathcal{S}_0 , the transition probability \mathcal{P} , reward function \mathcal{R} and the discount factor γ . $\mathcal{N} \equiv \{1, \dots, N\}$ is a set of N UAVs. $o_i = \mathcal{O}(s; i)$ denotes the observation for the UAV i under state $s \in \mathcal{S}$.

The goal of our work is to construct a policy that performs well across diverse scenarios. The task space \mathcal{T} defines a series of Dec-POMDPs with similar properties. We use a parameter space \mathcal{W} to represent the inter-task variation of \mathcal{T} . We generate the corresponding initial states by a task parameter $w \in \mathcal{W}$. In our setup, w comprises the initial positions of the UAVs and the evader, as well as the number and positions of obstacles. We consider homogeneous UAVs and learn a parameter-sharing policy π_θ parameterized by θ to output action $a_i \sim \pi_\theta(\cdot | o_i)$ for UAV i . The final objective $J(\theta)$ is to maximize the expected accumulative reward for any task parameter $w \in \mathcal{W}$, i.e.,

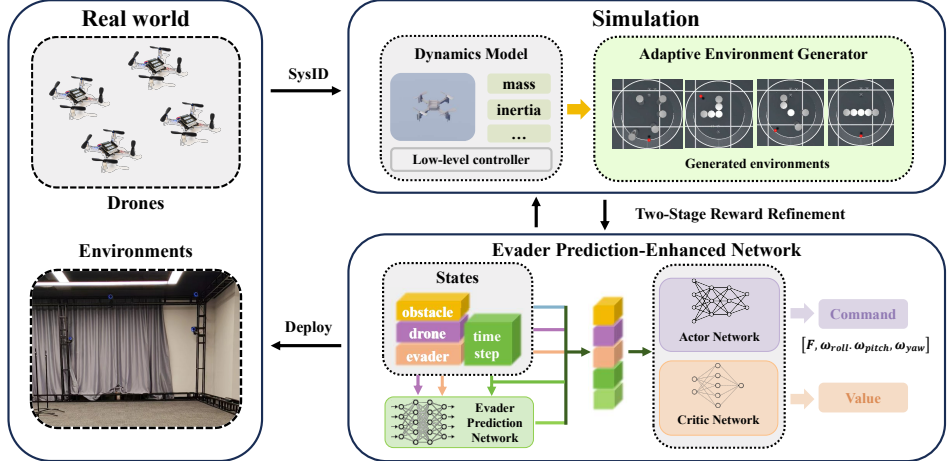


Fig. 2: Pipeline of our method. We begin by calibrating the parameters of the quadrotor dynamics model through system identification. Next, we introduce an *Adaptive Environment Generator* to automatically generate tasks for policy training and employ an *Evader Prediction-Enhanced Network* for efficient capture. Finally, with two-stage reward refinement, the learned policy is directly transferred to real quadrotors in a zero-shot manner.

$$J(\theta) = \mathbb{E}_{w \sim \mathcal{W}} [\sum_t \gamma^t R(s^t, \mathbf{a}^t; w) \mid w], \text{ where } \mathbf{a}^t \text{ is joint actions at timestep } t.$$

C. Quadrotor Model

In this paper, we use quadrotors, one of the most widely used UAV, as our physical platform. The quadrotor is assumed to be a 6 degree-of-freedom rigid body of mass m and diagonal moment of inertia matrix $\mathbf{I} = \text{diag}(I_x, I_y, I_z)$. The dynamics of the quadrotor are modeled by the differential equation: $\dot{\mathbf{x}} = [\dot{\mathbf{p}}^T, \dot{\mathbf{q}}^T, \dot{\mathbf{v}}^T, \dot{\boldsymbol{\omega}}^T]$, where the quadrotor state $\mathbf{x} \in \mathbb{R}^{13}$ consists the position \mathbf{p} , the orientation \mathbf{q} in quaternions, the linear velocity \mathbf{v} and the angular velocity $\boldsymbol{\omega}$. The acceleration of the quadrotor is described as

$$\ddot{\mathbf{v}} = \begin{bmatrix} 0 \\ 0 \\ -g \end{bmatrix} + R \begin{bmatrix} 0 \\ 0 \\ \sum_j \mathbf{f}_j / m \end{bmatrix}, \quad (1)$$

in the world frame with gravity g . \mathbf{f}_j is the force generated by the j -th rotor. R is the rotation matrix from the body frame to the world frame.

The angular acceleration calculated by Euler's rotation equation in the body frame is $\dot{\boldsymbol{\omega}} = \mathbf{I}^{-1}(\boldsymbol{\tau} - \boldsymbol{\omega} \times (\mathbf{I}\boldsymbol{\omega}))$. The torques $\boldsymbol{\tau}$ acting in the body frame are determined by $\boldsymbol{\tau} = \sum_j \boldsymbol{\tau}_j + \mathbf{r}_{pos,j} \times \mathbf{f}_j$, where $\boldsymbol{\tau}_j$ is the torques generated by the j -th rotor, $\mathbf{r}_{pos,j}$ is the position of the rotor j expressed in the body frame. We model the rotational speeds of the four motors Ω_j as first-order system with time constant T_m where the commanded motor speeds Ω_{cmd} are the input, i.e., $\dot{\Omega}_j = T_m(\Omega_{cmd,j} - \Omega_j)$. The force and torque produced by the j -th rotor are modeled as follows: $\mathbf{f}_j = k_f \Omega_j^2$, $\boldsymbol{\tau}_j = k_m \Omega_j^2$.

IV. METHODOLOGY

The pipeline of our method is shown in Fig. 2. To minimize the sim-to-real gap, we first calibrate the parameters of the quadrotor dynamics model via system identification, which are then integrated into the GPU-parallel simulator [30] to construct the multi-UAV pursuit-evasion task. We use collective thrust and body rates (CTBR) as control commands

and train RL policy to output it via a SOTA MARL algorithm, MAPPO [31]. To enhance active exploration under partial observability, we design an *Evader Prediction-Enhanced Network* that leverages an attention-based architecture to capture the interrelations within observations and a trajectory prediction network to forecast the evader's movement. To further enhance sample efficiency and policy generalization, we propose an *Adaptive Environment Generator* to automatically generate curricula, enabling efficient exploration of the entire task space. Finally, with reward refinement, the learned policy is applied directly to real quadrotors without any real data fine-tuning.

In the following sections, we first present the basic MARL setup, then detail the *Evader Prediction-Enhanced Network* architecture, the *Adaptive Environment Generator* design, and the two-stage reward refinement.

A. Multi-Agent Reinforcement Learning Setup

Observation Space. The observation \mathbf{o}_i for quadrotor i is composed of three components: the self-information \mathbf{o}_{self} , states of other quadrotors \mathbf{o}_{other} and information about obstacles \mathbf{o}_{ob} . \mathbf{o}_{self} consists of its orientation in quaternions, the linear velocity, the real and predicted future relative position to the evader. If the evader is not detected by any of the quadrotors, we mask the real relative position with a marker value. \mathbf{o}_{other} contains the relative positions to other quadrotors. \mathbf{o}_{ob} denotes the relative positions to the k -nearest obstacles, where k is smaller than the maximum number of obstacles, representing the quadrotor's inability to sense global information about environments.

Action Space. We adopt collective thrust and body rates (CTBR) commands as policy actions to ensure agile control, cooperative decision-making, and robust sim-to-real transfer. These CTBR commands are subsequently executed by a low-level PID controller. Concretely, the action for quadrotor i is expressed as $a_i = (F, \omega_{roll}, \omega_{pitch}, \omega_{yaw})$, where $F \in [0, 1]$ indicates the collective thrust, and $\omega \in [-\pi, \pi]$ signifies the body rates for the corresponding axes.

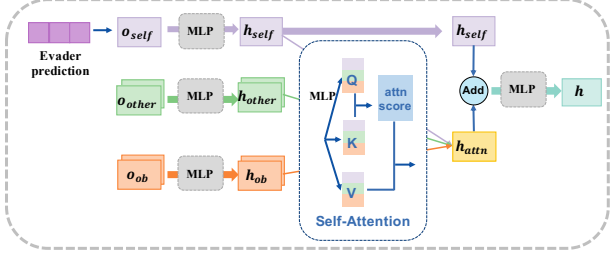


Fig. 3: Attention-based observation encoder.

Reward Function. The team-based reward function encourages quadrotors to capture the evader cooperatively while avoiding obstacles, consisting of four components: capture reward, distance reward, collision penalty, and smoothness reward. The capture reward motivates quadrotors to work together to capture the evader. If the evader falls within the capture radius of any quadrotor, all quadrotors receive a bonus of 2. The distance reward helps guide the quadrotor closer to the evader, applying a penalty, with a coefficient of -0.1 , proportional to the distance between the quadrotor and the evader. A collision penalty discourages quadrotors from getting too close to obstacles, imposing a significant penalty of -10 if they breach a safety threshold. Finally, the smoothness reward promotes stable and efficient quadrotor actions by encouraging minimal changes in control inputs between time steps. It is defined as $e^{-\|a^t - a^{t-1}\|}$, where $a^t - a^{t-1}$ represents the variation of commands output by the policy.

B. Evader Prediction-Enhanced Network

In the evader prediction-enhanced network, we first build an *Evader Prediction Network* that predicts the evader's future trajectories based on historical observations, facilitating the learning of cooperative pursuit strategies under partial observation. The predicted trajectories, concatenated with the raw observations, are then fed into the *Actor and Critic Networks*. These networks utilize an attention-based observation encoder to better capture the relationships between different entities.

1) *Evader Prediction Network*: We use an LSTM to predict the evader's trajectory for the next K timesteps. The input consists of n -step historical data, including the positions of all quadrotors, the positions and velocities of the evader, and the current timestep. If the evader is blocked by an obstacle and undetected by any quadrotor, we use a marker value to replace the evader's positions and velocities. To train the network, we collect data over $n + K$ timesteps during the rollout phase, using the first n timesteps as inputs X and the subsequent $n + 1$ to $n + K$ timesteps as labels Y . The evader prediction network P_ϕ is trained via supervised learning, and the loss is defined as $L_\phi = \mathbb{E}(Y - P_\phi(X))^2$.

2) *Actor and Critic Networks*: The actor and critic networks are based on the attention-based observation encoder, as illustrated in Fig. 3. The raw observation of quadrotor i consists of three components: \mathbf{o}_{self} , \mathbf{o}_{other} , and \mathbf{o}_{ob} . The predicted trajectory of the evader is concatenated into \mathbf{o}_{self} . Each component is separately encoded using distinct MLPs, producing embeddings of 128 dimensions each. A multi-head self-attention module is employed to capture the relationships between these embeddings, resulting in features \mathbf{h}_{attn} . To

Algorithm 1: Training with Adaptive Environment Generator

```

Input:  $\theta$ ,  $p$ ,  $\mathcal{Q}_{active}$ ,  $\sigma_{min}$ ,  $\sigma_{max}$ ;
Output: final policy  $\pi_\theta$ ;
 $\mathcal{Q}_{active} \leftarrow \{\}$ ;
repeat
    // Local expansion and global exploration.
     $W_{env} \leftarrow$  sample tasks from  $\mathcal{Q}_{active}$  with probability  $p$  and obtain expanded tasks  $w$  by Expand, else  $w \sim \text{Unif}(\mathcal{W})$  with probability  $1 - p$ ;
    // Train the policy  $\pi_\theta$ .
    Train and evaluate  $\pi_\theta$  with  $W_{env}$  via MARL;
    // select task parameters from  $W_{env}$ 
     $W_{new} \leftarrow \text{Selection}(W_{env}, \sigma_{min}, \sigma_{max})$ ;
    Add  $W_{new}$  to the active archive  $\mathcal{Q}_{active}$ ;
until  $\pi_\theta$  converges;

```

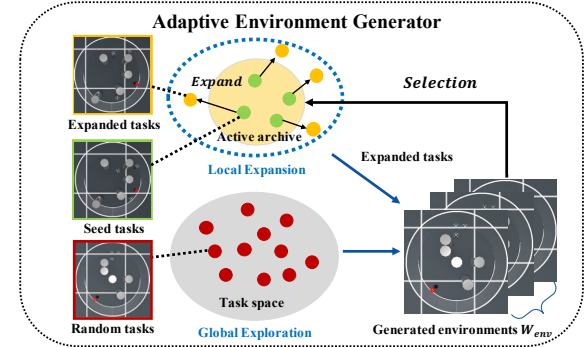


Fig. 4: Design of the *Adaptive Environment Generator*.

emphasize self-information, the self-embeddings \mathbf{h}_{self} are added to \mathbf{h}_{attn} and passed through an MLP to generate the final feature \mathbf{h} . In the actor network, actions are parameterized using a Gaussian distribution based on \mathbf{h} . For the critic network, \mathbf{h} is input into an MLP to produce a scalar value representing the estimated state value.

C. Adaptive Environment Generator

We aim to derive an RL policy that generalizes well to unknown environments. While domain randomization [32] is commonly used to improve generalization, directly randomizing task parameters requires a large number of samples and may struggle in complex tasks (see Sec. V-E). To address this, we propose an adaptive environment generator that efficiently navigates vast exploration space and integrates it into MARL training, as outlined in Algo. 1.

As shown in Fig. 4, we generate parallel simulation environments by *Local Expansion* and *Global Exploration*. The *Local Expansion* is responsible for improving the ability of quadrotors to effectively capture the evader from any starting position in a scenario with a fixed number and location of obstacles. We maintain an active archive \mathcal{Q}_{active} to store task parameters w of environments that the current policy still needs to solve. Then, we generate expanded tasks from *seed*

tasks sampling from the active archive by applying noise in the parameter space \mathcal{W} . We define the process of expansion as *Expand*. Specifically, for a particular seed task w , the expanded task is generated by introducing noise $\epsilon \in [-\delta, \delta]$ to the dimensions associated with both the quadrotors and the evader while leaving the obstacle-related dimensions unaltered. For the updating process of \mathcal{Q}_{active} , defined as *Selection*, we execute the current policy in the generated environments W_{env} and obtain a set C_{env} of task success rates for all environments. We introduce two hyper-parameters σ_{min} and σ_{max} and include the task parameters satisfying the criterion into the active archive \mathcal{Q}_{active} , i.e.,

$$\mathcal{Q}_{active} \leftarrow \{w | \sigma_{min} \leq c \leq \sigma_{max}, c \in C_{env}, w \in W_{env}\}. \quad (2)$$

Note that the hyper-parameters σ_{min} and σ_{max} are easy to tune due to their interpretation as bounds on the task success rate. In our setup, $\sigma_{min} = 0.5$ and $\sigma_{max} = 0.9$. The updating process of \mathcal{Q}_{active} continuously increases the complexity of tasks, leading to automatic curriculum generation.

The *Global Exploration* is used for continuous exploration of the entire task space, improving the ability of quadrotors to capture the evader under different obstacle placements. We randomly sample task parameters from the whole parameter space \mathcal{W} , i.e., randomly set up the initial positions of quadrotors and the evader, as well as the quantities and positions of obstacles. Finally, we select task parameters by *Local Expansion* with probability p , while those from *Global Exploration* are selected with probability $1 - p$. In our experiments, we choose $p = 0.7$.

D. Two-stage Reward Refinement

Since the reward function has multiple objectives, obtaining a feasible policy for real-world deployment is challenging. To ensure the policy meets physical constraints and is deployable in practice, we use a two-stage reward refinement process. Specifically, in the first stage, we initially exclude the smoothness reward and focus on the other three rewards. In the second stage, we gradually introduce the smoothness reward coefficient, ensuring a high success rate while improving the smoothness of actions.

V. EXPERIMENT

A. Experiment Setting

We construct the task using OmniDrones [30], a high-speed UAV simulator for RL policy training. The simulation environment, illustrated in Fig. 1b, is an arena with a radius of 0.9 and a maximum height of 1.2. The arena contains 4 to 5 randomly placed cylindrical obstacles, each with a radius of 0.1 and a height of 1.2. To avoid collisions, the distance between UAVs and between UAVs and obstacles must exceed 0.07. The setup includes 3 quadrotors, each with a maximum speed of 1.0, while the evader moves at a constant speed of 1.3. The capture radius is set at 0.3, and the maximum episode length is 800.

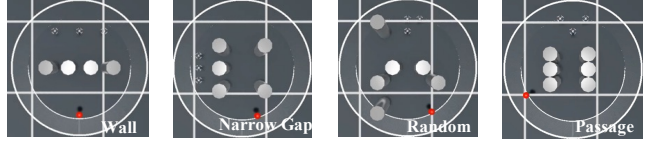


Fig. 5: Illustration of four test scenarios.

B. Evaluation

Evaluation Scenarios. We design four test scenarios (Fig. 5), illustrated in a top-down view. The within-distribution scenarios, *Wall* and *Narrow gap*, are intended to challenge the pursuit strategy. The two out-of-distribution scenarios, *Random* and *Passage*, are designed to evaluate the method's generalization to unseen environments.

Evaluation Metrics. We use three statistical metrics to evaluate pursuit strategies: Capture Rate, Capture Step, and Collision Rate. Each experiment is averaged over 300 testing episodes (100 per seed).

- **Capture Rate:** Percentage of successful episodes where the evader is captured before the maximum episode length. Higher values indicate better performance.
- **Capture Step:** Average timestep of first capture. If not captured, the maximum episode length is recorded. Lower values indicate quicker capture.
- **Collision Rate:** Average number of collisions between quadrotors and obstacles or other quadrotors per episode length. Lower values indicate safer pursuit.

C. Baselines

We challenge our method with three heuristic methods (Angelani, Janosov, and APF) and a RL-based method (DACOOP).

- **Angelani** [11]: Pursuers are attracted to the nearest particles of the opposing group, i.e., the evader.
- **Janosov** [12]: Janosov designs a greedy chasing strategy and collision avoidance system that accounts for inertia, time delay, and noise.
- **APF** [13]: APF guides pursuers to a target position by combining attractive, repulsive, and inter-individual forces. By setting the target of the pursuers to the evader's position and adjusting the hyperparameters for these forces, the pursuers can navigate towards the evader while avoiding obstacles.
- **DACOOP** [25]: DACOOP employs RL to adjust the primary hyperparameters of APF, enabling effective adaptation to diverse scenarios.

For heuristic methods, we perform grid search on hyperparameters in the training scenarios. For DACOOP, we use the same MARL algorithm (MAPPO) and hyperparameters as our approach. Baselines, treating the quadrotor as a point mass, outputs velocity commands executed by a velocity controller.

D. Simulation Results

Quantitative Results. Tab. I shows the performance across four test scenarios. In the *Wall* and *Narrow Gap* scenarios, our method achieves over 95% capture rate, with the lowest collision rate and fewest capture timesteps, demonstrating

Scenarios	Metrics	Angelani	Janosov	APF	DACOOP	Ours
Wall	<i>Cap. Rate</i> ↑	0.008(0.003)	0.009(0.002)	0.010(0.005)	0.205(0.007)	0.977(0.033)
	<i>Cap. Step</i> ↓	798.0(000.8)	797.0(000.8)	797.0(001.4)	744.0(009.1)	306.4(084.6)
	<i>Coll. Rate</i> ↓	0.010(0.000)	0.010(0.000)	0.010(0.000)	0.040(0.008)	0.000(0.000)
Narrow Gap	<i>Cap. Rate</i> ↑	0.213(0.012)	0.219(0.012)	0.253(0.012)	0.447(0.017)	0.953(0.037)
	<i>Cap. Step</i> ↓	755.0(004.5)	757.7(004.2)	743.0(002.2)	553.0(002.2)	510.1(131.6)
	<i>Coll. Rate</i> ↓	0.094(0.001)	0.077(0.001)	0.085(0.000)	0.039(0.002)	0.028(0.040)
Random	<i>Cap. Rate</i> ↑	0.277(0.002)	0.145(0.019)	0.314(0.018)	0.563(0.016)	1.000(0.000)
	<i>Cap. Step</i> ↓	639.0(001.6)	716.0(012.0)	620.0(014.8)	488.67(008.7)	315.7(069.6)
	<i>Coll. Rate</i> ↓	0.015(0.001)	0.018(0.002)	0.022(0.002)	0.020(0.000)	0.011(0.013)
Passage	<i>Cap. Rate</i> ↑	0.733(0.010)	0.009(0.003)	0.229(0.027)	0.818(0.027)	1.000(0.000)
	<i>Cap. Step</i> ↓	552.7(005.0)	799.3(000.5)	750.3(007.4)	533.7(008.8)	275.9(056.0)
	<i>Coll. Rate</i> ↓	0.000(0.000)	0.001(0.000)	0.001(0.000)	0.001(0.000)	0.006(0.008)

TABLE I: Results of all methods in test scenarios. Our approach significantly outperforms all baselines in unseen scenarios.

more effective cooperation in within-distribution tasks. In the *Random* and *Passage* scenarios, our method reaches a 100% capture rate, outperforming the baselines (56.3% and 81.8%) and requires the fewest capture steps. While the collision rate in *Passage* is slightly higher, it remains low at 0.6%. These out-of-distribution results show our policy’s strong generalization to unseen scenarios. We observe poor baseline performance and further test the algorithms in simpler, obstacle-free scenarios. Baselines show a sharp decline in the capture rate as the capture radius decreases, highlighting the difficulty of our task. In contrast, our method maintains a high capture rate, further proving its stronger cooperative capture ability. More analysis is available on our website.

Behavior Analysis. We observe four emergent behaviors in the test scenarios, which further illustrate the cooperative pursuit capabilities of our strategy. The corresponding video can be found in the supplementary materials. In *Wall* scenario, our approach achieves a double-sided surround strategy, where one quadrotor maintains surveillance while the other two approach the evader from both flanks. In contrast, baseline methods struggle to find a path to the evader quickly due to obstacles directly ahead. In *Narrow Gap* scenario, unlike the baselines, which continuously follow the evader, our approach learns to take a shortcut and intercept the evader at its inevitable path. In *Random* scenario, none of the drones detect the evader initially. Guided by the predicted evader trajectory, our method swiftly navigates behind obstacles, successfully locating the evader hidden there. In *Passage* scenario, our approach divides the quadrotors into three groups to block all possible escape routes for the evader. In contrast, baseline methods tend to greedily approach the evader, leaving an escape route open.

E. Ablation Studies

We conduct ablation studies on the core modules of our method, as shown in Fig. 6. “Ours w/o AEG” denotes the removal of the *Adaptive Environment Generator*, using random environment parameters instead. “Ours w/o EPN” refers to the removal of the *Evader Prediction Network*, where the RL

policy input lacks predicted trajectories. “MAPPO” indicates the removal of both the *Adaptive Environment Generator* and the *Evader Prediction Network*. Our method demonstrates the best sample efficiency, with an improvement of over 50%. “MAPPO” achieves only an 80% capture rate with 1.5 billion samples and exhibits large variance, highlighting the challenging nature of deriving an RL policy that considers UAV dynamics and performs well across diverse scenarios. “Ours w/o EPN” shows a lower capture rate, indicating that integrating evader trajectory prediction information into the RL policy input effectively guides UAVs to cooperatively capture the evader under partial observations. Although “Ours w/o AEG” achieves a comparable capture rate, it requires twice samples, demonstrating that the *Adaptive Environment Generator* significantly enhances sample efficiency.

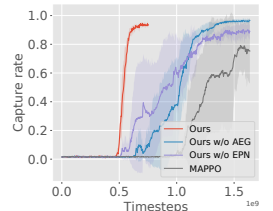


Fig. 6: Ablation studies. The graph shows the capture rate over time for four methods: "Ours" (red line), "Ours w/o AEG" (blue line), "Ours w/o EPN" (grey line), and "MAPPO" (black line). "Ours" shows the highest and most stable capture rate, reaching 1.0 quickly. "Ours w/o AEG" and "Ours w/o EPN" show comparable performance but slower than "Ours". "MAPPO" shows the lowest capture rate and highest variance.

F. Real-World Deployment

We further deploy the policy on three real CrazyFlie 2.1 quadrotors, each with a maximum speed limited to 1.0 m/s. A motion capture system is used to obtain the quadrotors’ states. We utilize a virtual evader and input its true states to the actor and the evader prediction network when the evader is detected. The actor and evader prediction network run on a local computer, which sends CTBR control commands at 100 Hz to the quadrotors via radio. Real-world experiments demonstrate that our method produces strategies consistent with those in the simulation, validating the feasibility of the capture policy on real quadrotors. A video is included in the supplementary materials.

VI. CONCLUSION

We learn a feasible RL policy that can perform online planning in unknown environment for multi-UAV pursuit-evasion and deploy it on real quadrotors. We introduce an *Adaptive Environment Generator* to automatically generate

curricula for policy generalization across diverse scenarios and employ an Evader Prediction-Enhanced Network for cooperatively capture. Simulations show our method significantly outperforms all baselines and generalizes to unseen scenarios. Future work will consider vision-based pursuit-evasion tasks.

REFERENCES

- [1] V. Turetsky and J. Shinar, "Missile guidance laws based on pursuit-evasion game formulations," *Automatica*, vol. 39, no. 4, pp. 607–618, 2003.
- [2] J. M. Eklund, J. Sprinkle, and S. S. Sastry, "Switched and symmetric pursuit/evasion games using online model predictive control with application to autonomous aircraft," *IEEE Transactions on Control Systems Technology*, vol. 20, no. 3, pp. 604–620, 2011.
- [3] D. W. Oyler, P. T. Kabamba, and A. R. Girard, "Pursuit–evasion games in the presence of obstacles," *Automatica*, vol. 65, pp. 1–11, 2016.
- [4] R. Vidal, O. Shakernia, H. J. Kim, D. H. Shim, and S. Sastry, "Probabilistic pursuit-evasion games: theory, implementation, and experimental evaluation," *IEEE transactions on robotics and automation*, vol. 18, no. 5, pp. 662–669, 2002.
- [5] D. Ye, M. Shi, and Z. Sun, "Satellite proximate pursuit-evasion game with different thrust configurations," *Aerospace science and technology*, vol. 99, p. 105715, 2020.
- [6] X. Fang, C. Wang, L. Xie, and J. Chen, "Cooperative pursuit with multi-pursuer and one faster free-moving evader," *IEEE transactions on cybernetics*, vol. 52, no. 3, pp. 1405–1414, 2020.
- [7] B. Tian, P. Li, H. Lu, Q. Zong, and L. He, "Distributed pursuit of an evader with collision and obstacle avoidance," *IEEE Transactions on Cybernetics*, vol. 52, no. 12, pp. 13512–13520, 2021.
- [8] H. Huang, W. Zhang, J. Ding, D. M. Stipanović, and C. J. Tomlin, "Guaranteed decentralized pursuit-evasion in the plane with multiple pursuers," in *2011 50th IEEE Conference on Decision and Control and European Control Conference*. IEEE, 2011, pp. 4835–4840.
- [9] A. Pierson, Z. Wang, and M. Schwager, "Intercepting rogue robots: An algorithm for capturing multiple evaders with multiple pursuers," *IEEE Robotics and Automation Letters*, vol. 2, no. 2, pp. 530–537, 2016.
- [10] R. Palm and A. Bouguerra, "Particle swarm optimization of potential fields for obstacle avoidance," in *Recent advances in robotics and mechatronics*, 2013, pp. 117–123.
- [11] L. Angelani, "Collective predation and escape strategies," *Physical review letters*, vol. 109, no. 11, p. 118104, 2012.
- [12] M. Janosov, C. Virág, G. Vásárhelyi, and T. Vicsek, "Group chasing tactics: how to catch a faster prey," *New Journal of Physics*, vol. 19, no. 5, p. 053003, 2017.
- [13] Y. Koren, J. Borenstein, *et al.*, "Potential field methods and their inherent limitations for mobile robot navigation," in *Icra*, vol. 2, no. 1991, 1991, pp. 1398–1404.
- [14] Z. Mu, J. Pan, Z. Zhou, J. Yu, and L. Cao, "A survey of the pursuit-evasion problem in swarm intelligence," *Frontiers of Information Technology & Electronic Engineering*, vol. 24, no. 8, pp. 1093–1116, 2023.
- [15] J. K. Gupta, M. Egorov, and M. Kochenderfer, "Cooperative multi-agent control using deep reinforcement learning," in *Autonomous Agents and Multiagent Systems: AAMAS 2017 Workshops, Best Papers, São Paulo, Brazil, May 8-12, 2017, Revised Selected Papers 16*. Springer, 2017, pp. 66–83.
- [16] S. F. Desouky and H. M. Schwartz, "Q (λ)-learning adaptive fuzzy logic controllers for pursuit–evasion differential games," *International Journal of Adaptive Control and Signal Processing*, vol. 25, no. 10, pp. 910–927, 2011.
- [17] M. D. Awheda and H. M. Schwartz, "The residual gradient facl algorithm for differential games," in *2015 IEEE 28th Canadian Conference on Electrical and Computer Engineering (CCECE)*. IEEE, 2015, pp. 1006–1011.
- [18] D. Luo, Z. Fan, Z. Yang, and Y. Xu, "Multi-uav cooperative maneuver decision-making for pursuit-evasion using improved madrl," *Defence Technology*, vol. 35, pp. 187–197, 2024.
- [19] W. Gan, X. Qu, D. Song, and P. Yao, "Multi-usv cooperative chasing strategy based on obstacles assistance and deep reinforcement learning," *IEEE Transactions on Automation Science and Engineering*, 2023.
- [20] Y. Wang, L. Dong, and C. Sun, "Cooperative control for multi-player pursuit-evasion games with reinforcement learning," *Neurocomputing*, vol. 412, pp. 101–114, 2020.
- [21] L. Xu, B. Hu, Z. Guan, X. Cheng, T. Li, and J. Xiao, "Multi-agent deep reinforcement learning for pursuit-evasion game scalability," in *Proceedings of 2019 Chinese Intelligent Systems Conference: Volume I 15th*. Springer, 2020, pp. 658–669.
- [22] M. Hüttenrauch, S. Adrian, G. Neumann, *et al.*, "Deep reinforcement learning for swarm systems," *Journal of Machine Learning Research*, vol. 20, no. 54, pp. 1–31, 2019.
- [23] N.-M. T. Kokolakis and K. G. Vamvoudakis, "Safety-aware pursuit-evasion games in unknown environments using gaussian processes and finite-time convergent reinforcement learning," *IEEE Transactions on Neural Networks and Learning Systems*, vol. 35, no. 3, pp. 3130–3143, 2022.
- [24] D. Liu, Q. Zong, X. Zhang, R. Zhang, L. Dou, and B. Tian, "Game of drones: Intelligent online decision making of multi-uav confrontation," *IEEE Transactions on Emerging Topics in Computational Intelligence*, 2024.
- [25] Z. Zhang, X. Wang, Q. Zhang, and T. Hu, "Multi-robot cooperative pursuit via potential field-enhanced reinforcement learning," in *2022 International Conference on Robotics and Automation (ICRA)*. IEEE, 2022, pp. 8808–8814.
- [26] R. Zhang, Q. Zong, X. Zhang, L. Dou, and B. Tian, "Game of drones: Multi-uav pursuit-evasion game with online motion planning by deep reinforcement learning," *IEEE Transactions on Neural Networks and Learning Systems*, 2022.
- [27] C. De Souza, R. Newbury, A. Cosgun, P. Castillo, B. Vidolov, and D. Kulic, "Decentralized multi-agent pursuit using deep reinforcement learning," *IEEE Robotics and Automation Letters*, vol. 6, no. 3, pp. 4552–4559, 2021.
- [28] V. Isler, S. Kannan, and S. Khanna, "Randomized pursuit-evasion in a polygonal environment," *IEEE Transactions on Robotics*, vol. 21, no. 5, pp. 875–884, 2005.
- [29] W. Gan, X. Qu, D. Song, and P. Yao, "Multi-usv cooperative chasing strategy based on obstacles assistance and deep reinforcement learning," *IEEE Transactions on Automation Science and Engineering*, pp. 1–16, 2023.
- [30] B. Xu, F. Gao, C. Yu, R. Zhang, Y. Wu, and Y. Wang, "Omnidrones: An efficient and flexible platform for reinforcement learning in drone control," *arXiv preprint arXiv:2309.12825*, 2023.
- [31] C. Yu, A. Velu, E. Vinitksy, Y. Wang, A. Bayen, and Y. Wu, "The surprising effectiveness of ppo in cooperative, multi-agent games," *arXiv preprint arXiv:2103.01955*, 2021.
- [32] J. Tobin, R. Fong, A. Ray, J. Schneider, W. Zaremba, and P. Abbeel, "Domain randomization for transferring deep neural networks from simulation to the real world," in *2017 IEEE/RSJ international conference on intelligent robots and systems (IROS)*. IEEE, 2017, pp. 23–30.